Stabilization of the Activated $\alpha_M\beta_2$ Integrin by a Small Molecule Inhibits Leukocyte Migration and Recruitment†

Mikael Björklund,‡,§ Olli Aitio,|| Michael Stefanidakis,‡,⊥ Juho Suojanen,⊥,#,△ Tuula Salo,△ Timo Sorsa,# and Erkki Koivunen*,‡

Department of Biological and Environmental Sciences, Viikinkaari 5D, POB 56, Faculty of Pharmacy, Drug Discovery and Development Technology Center, and Department of Oral and Maxillofacial Diseases, Helsinki University Central Hospital, Institute of Dentistry, University of Helsinki, Helsinki FI-00014, Finland, and Department of Diagnostics and Oral Medicine, Institute of Dentistry, University of Oulu, FI-90014 Oulu, Finland

Received November 2, 2005; Revised Manuscript Received January 12, 2006

ABSTRACT: Integrins are potential targets for the development of antiinflammatory agents. Here we develop a novel high-throughput assay by allowing a chemical library to compete with phage display peptide binding and identify a novel small-molecule ligand to the leukocyte-specific $\alpha_M\beta_2$ integrin. The identified thioxothiazolidine-containing compound, IMB-10, had an unexpected activity in that it stabilized binding of $\alpha_M\beta_2$ to its endogenous ligands proMMP-9 and fibrinogen. Single amino acid substitutions in the activity-regulating C-terminal helix and the underlying region in the ligand-binding I domain of the integrin suppressed the effect of IMB-10. A computational model indicated that IMB-10 occupies a distinct cavity present only in the activated form of the integrin I domain. IMB-10 inhibited $\alpha_M\beta_2$-dependent migration in vitro and inflammation-induced neutrophil emigration in vivo. Stabilization of integrin-mediated adhesion by a small molecule is a novel means to inhibit cell migration and may have a utility in treatment of inflammatory diseases involving leukocyte recruitment.

Integrins are a large family of heterodimeric cell surface receptors intimately involved in cell adhesion, migration, and signaling (*1*). Studies with the $\alpha_{IIb}\beta_3$ and $\alpha_V\beta_3$ integrins and the leukocyte-specific $\alpha_L\beta_2$ and $\alpha_M\beta_2$ integrins have been instrumental in understanding the integrin structure−function relationship (*2*−*8*). About half of the integrins, including the β_2 integrins, contain an inserted (I) domain in the α subunit as the major ligand-binding site, whereas those lacking the I domain use the α and β chains to form the ligand-binding pocket (*1*). There is a considerable clinical potential for compounds modulating integrin functions for the treatment of autoimmune diseases, inflammatory conditions, and cancer. As a result, small-molecule antagonists to the $\alpha_L\beta_2$ and other integrins have been identified (*9*−*12*). The α_L integrin targeting compounds are the best characterized group so far. These molecules stabilize the low-affinity conformation of the I domain and allosterically prevent ligand binding (*9*−*11*). Another class of small molecules bind to the integrin β_2 subunit I-like domain and prevent the activation of the α_L I domain, but at the same time they induce the active conformation of the β subunit I-like domain and the stalk domains (*6*). Additionally, two small-molecule antagonists of $\alpha_M\beta_2$ integrin have been identified in a high-throughput screening (*13*). These compounds inhibit, by an undefined mechanism, the binding of complement protein iC3b and fibrinogen, but not intercellular adhesion molecule (ICAM)-1, to the $\alpha_M\beta_2$ integrin (*13*).

Phage display has been widely adopted for the identification of short peptide ligands to numerous targets due to the simplicity and effectiveness of the method. We have previously identified a peptide ligand ADGACILWMDDGWCGAAG (DDGW)[1] to the α_M and α_L integrin I domains. The DDGW peptide mimics the integrin-binding sequence of the latent matrix metalloproteinases (proMMP)-2 and -9 and inhibits migration of leukocytes and leukocytic cell lines in vitro and leukocyte recruitment in vivo (*14*−*16*). Although a potent therapeutic activity for DDGW and many other phage display-derived peptides can be seen in animal models (*17*−*19*), rapid clearance, susceptibility to proteolysis, and

† This work was financially supported by grants from the Finnish Academy, Finnish Cancer Society, Finnish Cultural Foundation, and Helsinki University Central Hospital EVO (TYH 5306 and TI 020Y0002).

* To whom correspondence should be addressed. Tel: +358-9-19159023. Fax: +358-9-19159068. E-mail: erkki.koivunen@helsinki.fi.

‡ Department of Biological and Environmental Sciences, University of Helsinki.

§ Current address: Molecular and Cancer Biology Program, Biomedicum, University of Helsinki, Helsinki FI-00014, Finland.

|| Faculty of Pharmacy, Drug Discovery and Development Technology Center, University of Helsinki.

⊥ Equal contribution to this work.

Department of Oral and Maxillofacial Diseases, Helsinki University Central Hospital, Institute of Dentistry, University of Helsinki.

△ Department of Diagnostics and Oral Medicine, Institute of Dentistry, University of Oulu.

[1] Abbreviations: proMMP-9, latent matrix metalloproteinase-9; DDGW, ADGACILWMDDGWCGAAG peptide; GST, glutathione *S*-transferase; PDBu, 4β-phorbol-12,13-dibutyrate; uPAR, urokinase−plasminogen activator receptor; InhI, gelatinase-selective small-molecule inhibitor; LLG-C4-GST, CPCFLLGCC-peptide fusion with GST; DMSO, dimethyl sulfoxide; MTT, 3-(4,5-dimethylthiazol-2-yl)-2,5-diphenyltetrazolium bromide; TBS, Tris-buffered saline; PBS, phosphate-buffered saline; ICAM, intercellular adhesion molecule; BSA, bovine serum albumin; TG, thioglycolate; EDTA, ethylenediaminetetraacetic acid.

10.1021/bi052238b CCC: $33.50
Published on Web 02/09/2006

immunogenicity may limit the utility of such peptides as therapeutic agents in human diseases. To overcome these limitations, competition assays utilizing labeled peptides have been developed to identify functionally similar small molecules (*20*, *21*). However, these approaches may suffer from the effects of labeling reagents on the biological activity of the peptide and from the lack of sensitivity, thus requiring considerable assay optimization. We have here utilized the fast and sensitive phage assay to screen for small-molecule compounds that would inhibit DDGW peptide binding to the $\alpha_M\beta_2$ integrin. We discover a novel class of small-molecule integrin ligands, and the representative compound possessed potent antiinflammatory activity in a mouse model.

METHODS

Screening of a Compound Library. A combinatorial library of 10000 small molecules and the follow-up compounds were purchased from ChemBridge (San Diego, CA). A competition assay with the DDGW peptide bearing phage was set up by immobilizing 20 ng per well of recombinant α_M I domain−GST fusion in 96-well plates (*22*). The bacterially expressed α_M and α_L I domain−GST fusions bind most endogenous ligands in the absence of the integrin β subunit and can be immobilized on plastic without a loss of activity. The compounds were assayed in pools of eight compounds, each at a 5 μM concentration and dimethyl sulfoxide (DMSO) as a solvent at a 1.25% concentration. After preincubation of the compounds in duplicate wells, DDGW phage was added at 3×10^8 transducing units per well. Soluble DDGW peptide, a control peptide, and an irrelevant phage were included in every plate as controls and to subtract the background binding. Phage binding was determined with an anti-phage antibody as described (*23*). When retested as single compounds at a 5 μM concentration, those with at least 50% inhibition were considered positive. The structures of these hits and their DDGW phage inhibiting activities are reported in Supporting Information. To calculate the IC_{50} values, the dilution series of the DDGW peptide and compounds (10 μM to 150 nM) were tested in the DDGW phage assay.

In Vitro Binding Assays. The catalytically inactive proMMP-9-ΔHC-E^{402}Q mutant was prepared via site-directed mutagenesis and purified using gelatin−Sepharose (*23*). The resulting MMP-9 with this mutation is structurally identical to the wild-type protein (*24*). ProMMP-9-ΔHC-E^{402}Q, intact proMMP-9, or fibrinogen (100 ng per well) was coated on microtiter wells in TBS followed by saturation of the wells with 1% BSA in PBS/0.05% Tween-20. Soluble α_M integrin I domain−GST fusion protein (2.5 μg/mL) was added with or without the peptides or compounds in 0.1% BSA/TBS/0.05% Tween-20/1 mM $CaCl_2$/1 mM $MgCl_2$ and incubated for 1 h. Bound protein was detected with anti-GST antibody (1:2000 dilution) and peroxidase-conjugated anti-goat antibody (1:2000 dilution). The mutant α_M I domains were prepared with site-directed mutagenesis, and their integrity was confirmed with DNA sequencing. The anti-GST antibody bound equally well to the purified proteins with less than 5% difference between the mutants.

To study whether the compounds compete with the binding of integrin I domain-specific antibodies, α_M I domain−GST, α_L I domain−GST, or GST (each 2 μg/mL) was bound to microtiter wells via the GST domain. After washing, the anti-I domain monoclonal antibodies or control IgG (2 μg/mL) was subjected to the I domains in the presence of IMB-10 (2 μM), IMB-8, or DMSO. Bound antibody was detected with peroxidase-conjugated anti-mouse antibody (1:2000 dilution). Control IgG or GST alone gave no binding. The LM2/1 and MEM170 recognize the α_M I domain, whereas the TS1/22 and MEM83 are specific for the α_L I domain (*6*, *18*, *25*). The assay with purified $\alpha_M\beta_2$ integrin was done similarly except that the integrin (50 ng per well) was directly coated on microtiter wells.

Cell Culture. THP-1 monocytic leukemia, OCI-AML-3 acute myeloid leukemia, U937 histiocytic lymphoma, and HT1080 fibrosarcoma cells were cultured as described (*15*, *17*, *18*). The cell viability in the presence of the compounds or DMSO as a vehicle for 48 h was measured using a 3-(4,5-dimethylthiazol-2-yl)-2,5-diphenyltetrazolium bromide (MTT) assay as described (*23*).

Cell Adhesion and Migration. Cell adhesion experiments were performed as described (*18*). Briefly, THP-1 cells (50000 per well) were stimulated with 50 nM PDBu (4β-phorbol-12,13-dibutyrate; Sigma-Aldrich) and allowed to bind to fibrinogen-coated microtiter wells (10 μg/mL) in the presence or absence of compounds or DMSO in serum-free RPMI medium containing 0.1% BSA. Nonadherent cells were removed by gentle washing with PBS or 2.5 mM EDTA in PBS, and adherent cells were quantified with a phosphatase assay (*18*). Alternatively, THP-1 and U937 cells were stimulated with PDBu and allowed to adhere on uncoated plastic overnight. Nonadherent cells were removed by washing with PBS followed by six washes with 2.5 mM EDTA in PBS. Cell migration was done using transwells (5 μm pore size) coated with 40 μg/mL LLG-C4-GST or fibrinogen (*18*). THP-1 and OCI-AML-3 cells (50000 cells/100 μL) were allowed to migrate overnight in 10% FBS/RPMI medium in the presence or absence of peptides or compounds and 40 nM PDBu. Gelatinase-selective inhibitor I (InhI) at a 50 μM concentration (Calbiochem) was used to evaluate the level of gelatinase-dependent migration on fibrinogen. Migrated cells were stained with crystal violet and counted (*18*). Migration of HT1080 cells on serum-coated transwells was conducted as described (*17*).

Cellular Cleavage of the Urokinase−Plasminogen Activator Receptor. Pericellular gelatinase-dependent uPAR cleavage was performed as described (*23*). Briefly, OCI-AML-3 cells were stimulated with PDBu or left untreated and cultured for 48 h in the presence of 20 μM IMB-10, the gelatinase-selective inhibitor (InhI), or vehicle (DMSO). uPAR and its cleaved form uPAR D2+3 were detected with western blotting using a polyclonal antibody to uPAR (399R; American Diagnostica).

Computational Modeling. The C-terminal residues from N^{310} to K^{315} from the X-ray structure of the α_M I domain in the open conformation [PDB code 1m1u (*26*)] were deleted and substituted with residues N^{310} to A^{318} in the conformation of the closed structure [PDB code 1jlm (*27*)]. The C-terminal helix in the closed structure extends from E^{303} to A^{318}, suggesting that a similar helical structure is possible in the open structure. The substitution was carried out by superimposing the Cαs of amino acids Q^{309} to Q^{311} of the open and closed structures and by bonding the carbonyl C of Q^{309} in the open structure to the amide N of N^{310} of the terminal

peptide of the closed structure. The ϕ angles of N^{301} and F^{302} were rotated arbitrarily by 5.5° and by 6° to −91° and to −65°, respectively, to increase the size of the hydrophobic socket. These modifications are small as the C-terminal helix is known to be highly flexible. The Cβ−Cγ bond of K^{166} was rotated by 139° to −59° in order to avoid overlap with the C-terminal helix. Hydrogens were added to the protein, and the structure was energy minimized in SYBYL 7.0 (Tripos, St. Louis, MO) using the TRIPOS force field. A total of 100 iterations using the conjugate gradient method were performed. The minimized structure was used for ligand docking. Ligand geometry was optimized using the semi-empirical AM1 method in Spartan 5.1.3 (Wavefunction Inc., Irvine, CA). The docking experiments were performed using AUTODOCK3.0 (*28*). Gasteiger−Hückel partial charges were calculated in SYBYL7.0 for protein and ligand. Grid maps with 60 × 60 × 60 points and a grid-point spacing of 0.375 Å centered in the hydrophobic socket near I^{236} were calculated. The phenylbutadienyl moiety of the ligand was constrained to all-trans conformation during docking. Fifty separate docking simulations were performed using the Lamarckian genetic algorithm. The α_L I domain was generated from the cysteine-constrained high-affinity structure [PDB code 1mq9 (*29*)] so that the cysteines were replaced by the original lysine amino acids and the energy was minimized as with the α_M I domain.

Neutrophil Emigration in Vivo. The mouse experiments were approved by the ethical committee for the animal experiments at the University of Helsinki. Inflammation was induced in BALB/cOlaHsd female mice maintained in the Viikki Laboratory Animal Centre by injecting 1 mL of 4% thioglycolate broth in PBS ip, followed by intravenous injections of chemicals (200 μL at a 20 μg/mL concentration) or PBS after 5 min. Cells emigrated in the peritoneum after 3 or 24 h were counted using a hemocytometer.

Statistical Analysis. The statistical significance between groups in the peritonitis model was calculated with one-way ANOVA and differences found were analyzed by Bonferroni pairwise multiple comparison tests. Results with $p < 0.05$ were deemed significant.

RESULTS

High-Throughput Phage Binding Assay. We developed a simple competition assay where compounds from a small-molecule library are allowed to compete with a peptide-bearing phage for binding to an immobilized target protein. We specifically wanted to avoid the use of synthetic peptides in the assay owing to potential effects of labeling reagents on the biological activity of the peptide and from the potential lack of sensitivity. However, as phage-displayed peptides may sometimes be difficult to displace in binding assays due to avidity effects, we used the pIII minor coat protein present at two to five copies per phage for peptide display and preincubated the chemicals with the target before adding the phage to minimize the avidity effects. The bound phage is detected with an antibody recognizing the major coat protein of the filamentous bacteriophage. As the major coat protein is present in about 2500 copies, this significantly improves the sensitivity of our assay. Hence, a decrease in phage binding is a direct measure of competition between the binding of the chemical compound and the phage-displayed peptide.

We utilized this technique to identify small-molecule binders to the integrin α_M I domain using phage displaying the DDGW peptide. Of 10000 compounds screened, 19 (0.2%) showed significant and reproducible inhibition of DDGW-phage binding. Fourteen compounds had a common 2-thioxothiazolidin-4-one substructure [Figure 1A; all positive compounds are shown in Figure S1 (see Supporting Information)]. The identified compounds specifically inhibited DDGW-phage binding to the α_M I domain but had no effect on the binding of two other phage-displayed peptides, the CRVYGPYLLC and CGYGRFSPPC peptides to the C-terminal and the collagen-binding domain of MMP-9, respectively (ref *23* and data not shown). The representative compounds IMB-2, -6, -8, and -10 were tested to measure their IC_{50} values for the inhibition of DDGW-phage binding to the α_M I domain (Figure 1B). The activity difference between the most active compound, IMB-10, and the weakly active IMB-8 was over 20-fold. Most compounds were also more active than the DDGW peptide in this assay. The least active compound, IMB-8, was much less active than the DDGW peptide in phage assay and was essentially inactive in other assays at the concentrations used. Hence, it is unlikely that we have missed the identification of any potent lead compounds. IMB-10 and the other compounds identified in this screen also inhibited DDGW-phage binding to the α_L I domain (not shown). Because the DDGW peptide binds less efficiently to the α_L than the α_M I domain (*15*), we could not, however, reliably quantitate the activity of the identified compounds to the α_L I domain in the phage-binding assay.

To show that the identified chemicals specifically recognize the I domain, we studied their ability to inhibit binding of known I domain-specific monoclonal antibodies. At a 2 μM concentration IMB-10 inhibited binding of the α_M I domain-specific antibodies LM2/1 and MEM170 to recombinant α_M I domain by 33% and 40%, respectively (Figure 1C). The IMB-8 was only slightly active in this assay. The IMB-10 similarly inhibited LM 2/1 antibody binding to purified $\alpha_M\beta_2$ (Figure 1C, inset). Binding of TS1/22 antibody to the α_L I domain was strongly inhibited by IMB-10, but not by IMB-8, indicating that IMB-10 also recognizes the α_L I domain (Figure 1D). Another α_L I domain recognizing antibody, MEM83, was also significantly inhibited by IMB-10. As a control, the compounds did not inhibit GST antibody binding to the α_M I domain−GST fusion (Figure 1D, inset).

IMB-10 Increases Ligand Binding by the α_M I Domain in Vitro. We next tested if the compounds could also inhibit binding of the α_M I domain to its endogenous ligands proMMP-9 and fibrinogen. To test proMMP-9 binding, we prepared a catalytically inactive mutant proMMP-9-E^{402}Q-ΔHC, which lacks the collagen V-like "hinge" region and the C-terminal domain and does not autodegrade. The α_M I domain−GST fusion bound native proMMP-9 and proMMP-9-E^{402}Q-ΔHC equally well, demonstrating that MMP catalytic activity is not needed for this interaction (Figure 2A). Surprisingly, although the compounds inhibited phage and antibody binding to the α_M I domain, they greatly enhanced the binding of proMMP-9 and fibrinogen (Figure 2B). This observation was in striking contrast to the activity of the DDGW peptide, which inhibited ligand binding. The activities of the compounds correlated with their IC_{50} values in the phage assay, IMB-10 enhancing the binding the most. This effect was also observed with native proMMP-9 (not

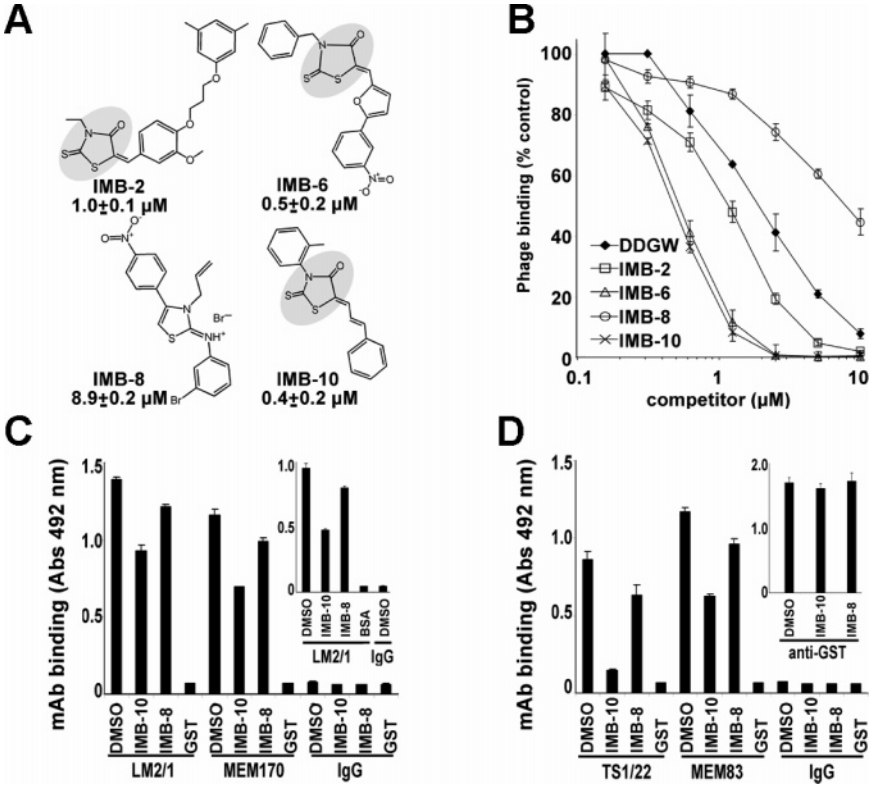

FIGURE 1: Identification of novel α_M integrin I domain-binding chemicals. (A) Representative structures of the α_M I domain-binding compounds and their IC_{50} values in the DDGW-phage assay are shown. The thioxothiazolidinone core structure is shaded with gray. (B) Results of the DDGW-phage assay where the IC_{50} values of the compounds indicated in (A) were measured. (C) Competition of binding of α_M integrin-specific antibodies. Antibody binding to the recombinant α_M I domain−GST fusion or GST control protein was measured in the presence of compounds (2 μM) or vehicle (DMSO). Inset: LM2/1 antibody binding to purified $\alpha_M\beta_2$ integrin. BSA denotes wells coated with BSA only. (D) Competition of binding of α_L integrin-specific antibodies as above. Inset: Anti-GST antibodies were used to recognize the α_M I domain−GST. The data shown in these and other figures are the mean ± SD from a representative experiment assayed in triplicate.

shown). We conclude that the compounds show a novel activity by enhancing the ligand-binding activity of the recombinant α_M I domain and differ from the previously identified small-molecule ligands of the α_L I domain, which inhibit ligand binding (*26*, *30*).

The activation state of the integrin I domains is regulated by the movement of the C-terminal helix resulting in a "closed" low-affinity or "open" high-affinity conformation (*26*, *27*, *31*). To gain insight into the binding site of IMB-10, we prepared α_M I domain mutants and tested their binding activity in the presence of chemicals. The $I^{236}A$ and $Y^{267}A$ mutations target the hydrophobic socket that controls the activation state of the I domains by accommodating the side chain of I^{316}, which is absolutely conserved in the C-terminal helix of all integrin I domains and which functions to maintain the I domain in the closed conformation (*26*). The I^{308} and L^{312} residues in the C-terminal helix and the conserved Y^{267} residue under this helix were mutated to alanine as the corresponding residues in the α_L I domain are within a 4 Å distance from the receptor-bound lovastatin (*32*). The K^{245} located in the vicinity of the metal ion-dependent adhesion site was selected for analysis as this residue has been speculated to be an important residue for proMMP-9 binding (15) and is also a critical determinant for the high-affinity binding of iC3b (*33*).

Binding of the mutant α_M I domains to proMMP-9-E^{402}Q-ΔHC and fibrinogen revealed that all of the mutants, especially $I^{236}A$ and $Y^{267}A$, were induced less by IMB-10 compared to the activation observed in the wild-type protein (Figure 2C). The basal binding activity of the $I^{308}A$ and $L^{312}A$ mutants was higher than that of the wild-type protein, similarly to that observed with the $I^{316}G$ mutant (*26*), but their binding could still be induced by IMB-10. The $K^{245}A$ mutant binding to proMMP-9-E^{402}Q-ΔHC was hardly inducible by IMB-10, confirming that this site is critical for high-affinity binding to proMMP-9. The locations of the mutated residues in the structure of the α_M I domain are shown in Figure 3A.

Modeling of IMB-10 Binding. As it is a considerable challenge to purify sufficient amounts of active $\alpha_M\beta_2$ integrin for direct biophysical characterization of a compound's binding, we set to study the binding site of IMB-10 using a computational modeling approach. Because the C-terminal α-helix is involved in crystal contacts in the open structure (*27*, *34*), we replaced the most distal part of it with that observed in the X-ray structure of the closed conformation (see Methods). Examination of the resulting model shows a discernible hydrophobic cavity underneath the C-terminal helix as also observed previously (*35*). As discussed above, this cavity is occupied by the I^{316} and L^{312} residues in the closed structure. We slightly increased the size of the hydrophobic cavity by rotating the ϕ angles of N^{301} and F^{302} residues. Docking using this model indicated that the elongated structure of IMB-10 fits well into the hydrophobic

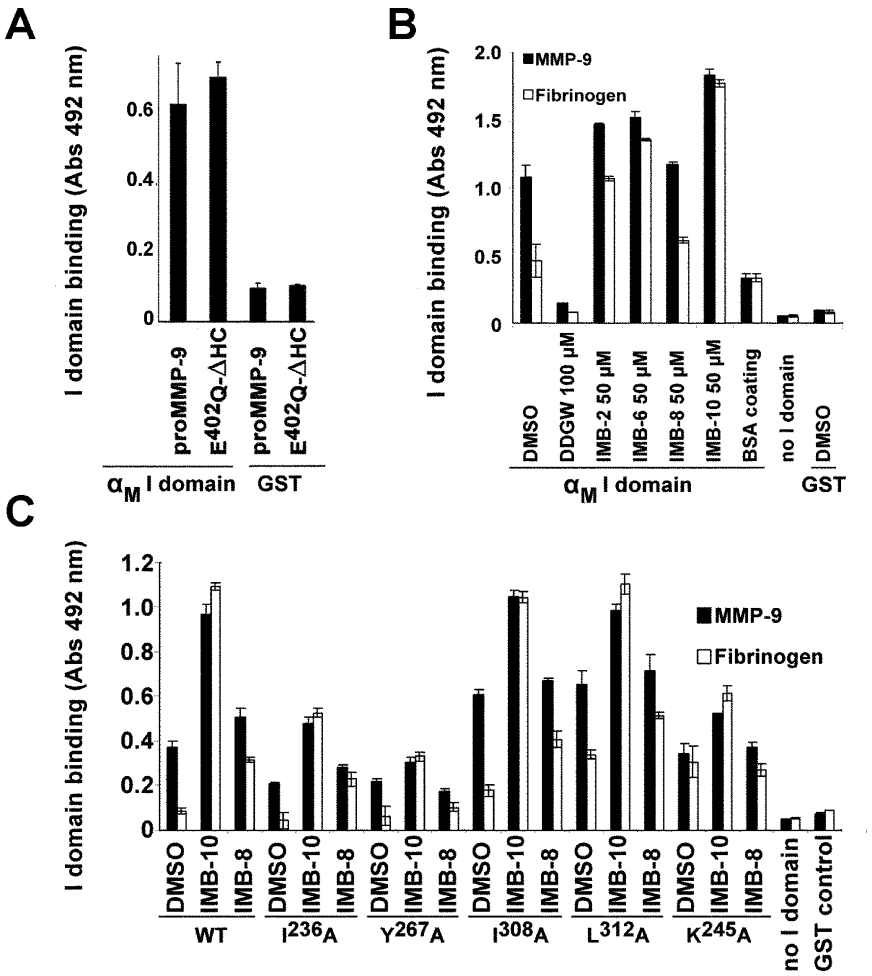

FIGURE 2: The identified chemicals do not inhibit but rather enhance the ligand binding ability of the α_M integrin. (A) The α_M I domain−GST fusion recognizes both wild-type proMMP-9 and the catalytically inactive, C-terminally truncated proMMP-9-E^{402}Q-ΔHC. Wild-type GST is used as a control. The bound GST protein was measured. (B) Binding of α_M I domain−GST to proMMP-9-E^{402}Q-ΔHC, fibrinogen, or BSA in the presence of DDGW peptide (100 μM), the indicated compound (50 μM), or vehicle (DMSO). (C) Effects of α_M I domain mutations on the activities of chemicals. Binding to proMMP-9-ΔHC-E^{402}Q and fibrinogen was measured as above. Background BSA binding is deducted. The data shown are mean ± SD from samples assayed in triplicate.

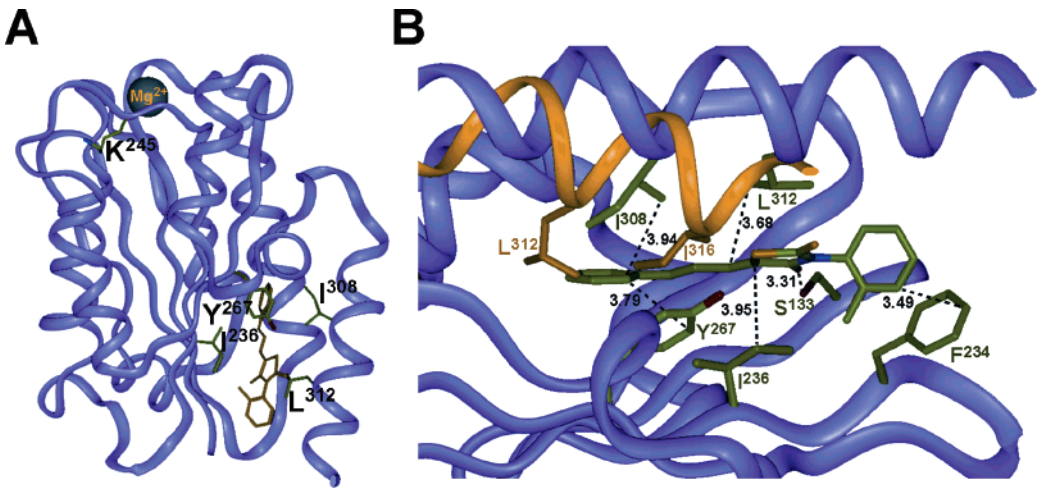

FIGURE 3: Modeling of an IMB-10 binding site. (A) Binding of IMB-10 into the open conformation of the α_M I domain. The side chains of mutated residues and the metal ion (Mg^{2+}) are marked. (B) Detailed view into the hydrophobic cavity of the open conformation with the bound IMB-10. The I domain shown in (A) was rotated 90° counterclockwise. Residues providing contacts with IMB-10 and their distances in angstroms are indicated with green and black, respectively. For comparison, the C-terminal helix of the superimposed closed conformation is shown (in yellow).

groove underneath the C-terminus so that the I^{308} and L^{312} residues form contacts with IMB-10 (Figure 3). We could not find any other satisfactory binding site for IMB-10 in either the closed or open conformation. As can be seen, the

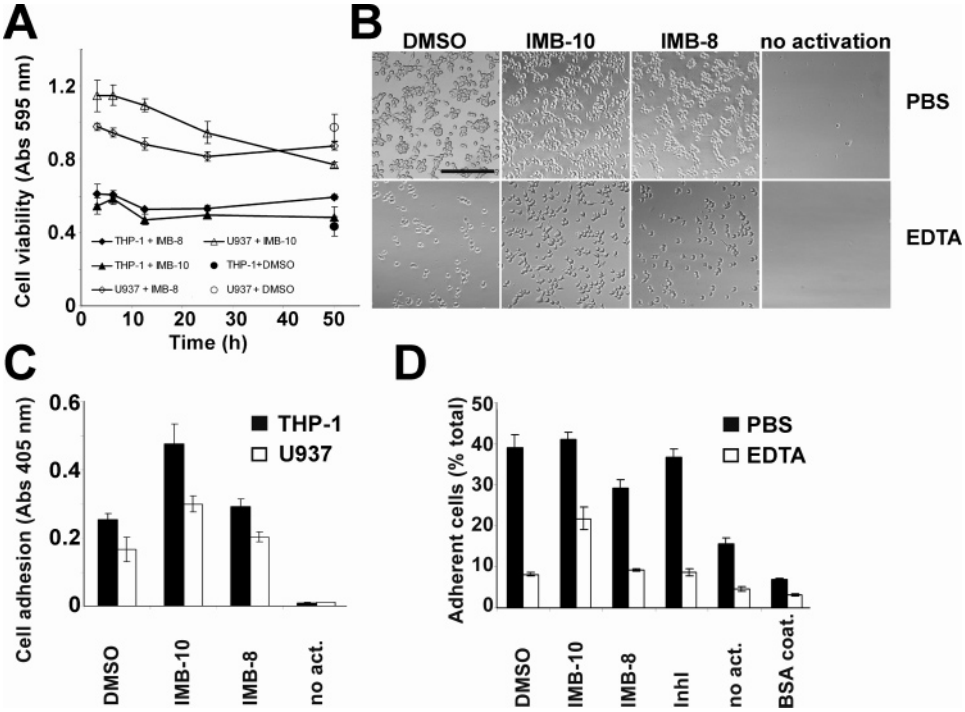

FIGURE 4: Stabilization of β_2 integrin-mediated cell adhesion by IMB-10. (A) The effect of the chemicals on the viability of THP-1 and U937 cells was studied using the MTT assay. Samples were analyzed at the indicated time points. DMSO control is shown for both cell lines. (B) Effects of the chemicals (25 μM) on adhesion of PDBu-activated or nonactivated THP-1 cells on plastic. Cells that remained attached after washing with PBS or 2.5 mM EDTA in PBS were photographed. Bar = 200 μM. (C) Quantitation of the chemical-induced highly adherent THP-1 and U937 cells that resist washing with EDTA. Cells remaining adherent were determined using a phosphatase assay. No act. = no PDBu activation. (D) Quantitation of THP-1 cells bound to fibrinogen after PBS or EDTA washings. The adherent cells were quantified by comparing to the phosphatase activity of known amounts of cells added to the wells.

proposed binding site of IMB-10 is completely blocked by the hydrophobic side chains of the C-terminal helix in the closed conformation (Figure 3B).

Our model indicates that all of the side chains which we mutated, except for the K^{245}, are within a 4 Å distance from IMB-10 and thus able to form intermolecular contacts with the chemical. Importantly, the bulky phenylbutadienyl moiety occupies the bottom of the cavity to which the Y^{267}, I^{236}, and I^{308} residues provide shape. Further contacts are between the 2-methylphenyl group of IMB-10 and the aromatic ring of F^{234}. The carbonyl group of the thioxothiazolidine ring, which is the only group of the molecule being able to participate in H-bonds, points toward the hydroxyl group of S^{133}, providing a possible explanation why the thioxothiazolidine-containing compounds were preferentially identified in the screen. Comparison of the α_M I domain model with that of the α_L I domain shows significant differences. Although a similar cavity is present in the open conformation of the α_L I domain and is sufficiently large to accommodate IMB-10, it provides much poorer complementary surface (Figure S2).

To perform an initial structure−activity relationship analysis, we examined compounds similar to IMB-10. Phage assay was conducted with these and related compounds identified in the primary screen (Figure S3). The results indicated that modifications in the phenylbutadienyl "tail" region of IMB-10 which occupies the bottom of the proposed binding cavity result in a substantial decrease in activity, whereas additions in the other end were better tolerated, except for a hydroxyl group in the para position, which based on the model would result in an unfavorable interaction with the F^{234} residue of the I domain. Finally, a short analogue to IMB10, which has only a single carbon instead of the three carbon "linker", was inactive, indicating that the overall length of the IMB-10 is critical for optimal activity.

Cells Treated with IMB-10 Are Strongly Adherent and Have Migration Defects. In the cell culture, IMB-10 and IMB-8 had only a minor effect on U937 cell proliferation at a 50 μM concentration but had no effect at all on other leukocytic cells, such THP-1 cells (Figure 4A) or OCI-AML-3 cells, or nonleukocytic cells, such as HT1080 fibrosarcoma cells (not shown). A 25 μM concentration, which showed no apparent toxicity, was used as a maximal concentration in the following cell-based assays.

Adhesion to uncoated cell culture plastic is a hallmark of $\alpha_M\beta_2$ integrin activity (*36*). THP-1 cells that were cultured on plastic in the presence of phorbol ester (PDBu) adhered strongly and were not detached by washing with PBS (Figure 4B). The cells could be detached with 2.5 mM EDTA, which counteracts the divalent cation-dependent adhesion. Interestingly, a significant portion of the IMB-10-treated cells remained adherent, resisting the effect of EDTA (Figure 4B,C). IMB-8 had no such an effect. The U937 histiocytic lymphoma cells stimulated with PDBu adhered on plastic less strongly than THP-1 cells, but an increased adhesion was similarly induced by IMB-10 but not IMB-8 (Figure 4C). The effect of IMB-10 was not restricted to adhesion on plastic but was also observed using fibrinogen as a substratum (Figure 4D). Similar results were obtained with $\alpha_M\beta_2$ integrin-dependent adhesion of OCI-AML-3 cells on fibrinogen, whereas $\alpha_V\beta_3$ integrin-mediated adhesion of HT1080 fibrosarcoma cells on fibrinogen was unaffected by the chemicals (not shown). In the absence of phorbol ester activation, IMB-10 did not stimulate cell adhesion, suggest-

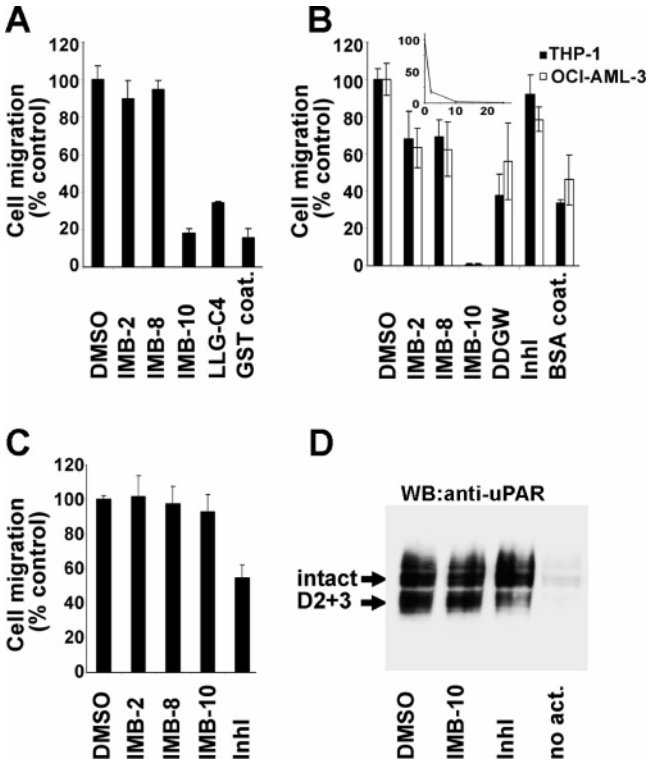

FIGURE 5: The IMB-10 compound is a potent inhibitor of leukemia cell migration. (A) Migration of THP-1 cells on LLG-C4-GST coated transwells in the presence of the indicated compounds (25 μM) or soluble LLG-C4 peptide (100 μM). Cell migration on GST coating is shown as a control. (B) Migration of THP-1 and OCI-AML-3 cells using fibrinogen or BSA coating. The DDGW peptide was 200 μM and the gelatinase-selective small-molecule inhibitor InhI 50 μM. Inset: dose-dependent inhibition of OCI-AML migration on fibrinogen by IMB-10. The *X*-axis is the IMB-10 concentration in μM. (C) Migration of HT1080 fibrosarcoma cells on serum-coated transwells in the presence of competitors as in (B). The results are representative from two to three experiments. (D) Pericellular proteolysis of urokinase−plasminogen activator receptor (uPAR). OCI-AML-3 cells were stimulated with PDBu in the presence of 20 μM IMB-10, the gelatinase-selective inhibitor (InhI), or vehicle (DMSO) or left untreated. uPAR and the cleavage product uPAR D2+3 were detected with western blotting.

ing that IMB-10 stabilizes the active α_M I domain rather than activates it.

As the DDGW peptide was previously shown to inhibit cell migration (*14*, *15*), the effect of the compounds on cell migration was evaluated in a transwell assay. THP-1 cells migrate on a LLG-C4-GST substratum in a β_2 integrin-dependent manner (*18*). In this assay, IMB-10 potently inhibited cell migration as did a soluble LLG-C4 peptide (Figure 5A). The less active compounds IMB-2 and -8 did not inhibit the cell migration at a 25 μM concentration. On a fibrinogen matrix, IMB-10 completely inhibited migration of THP-1 and OCI-AML-3 cells at a 25 μM concentration, whereas IMB-2 and -8 were much less active (Figure 5B). An inhibitory effect was also obtained by the DDGW peptide but not by the gelatinase inhibitor InhI. The α_M I domain binding chemicals did not have any effect on β_2 integrin-independent cell motility of HT1080 cells, which was partially inhibited by the gelatinase-selective inhibitor InhI (Figure 5C).

In addition to integrin function, proteolytic activity significantly contributes to the rate of cell migration. As proMMP-9 interacts with $\alpha_M\beta_2$ integrin on the cell surface

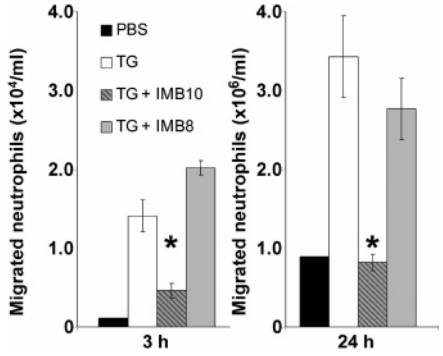

FIGURE 6: IMB-10 inhibits leukocyte recruitment in vivo. Thioglycolate (TG) was used to induce peritonitis in mice. PBS was used as a control. The mice received IMB-8 or IMB-10 as an intravenous injection. Cells migrated to the peritoneal cavity were collected after 3 or 24 h and counted. The data shown are mean ± SEM (n = 5). The statistical difference between the TG injected mice was studied with ANOVA, and the observed differences between the groups were compared using the Bonferroni test. An asterisk indicates a statistical significance (p = 0.001, in 4 h experiment, and p = 0.01 in 24 h experiment).

(*14*, *15*), we wished to evaluate the effect of IMB-10 on pericellular gelatinase activity. The proteolysis of urokinase−plasminogen activator receptor (uPAR) has been shown to depend on gelatinase activity (*23*). Furthermore, uPAR interacts with $\alpha_M\beta_2$ integrin through a non-I domain binding site (*37*). OCI-AML-3 cells stimulated with phorbol ester had a high level of intact uPAR and the uPAR D2+3 cleavage product. The cleavage of uPAR could not be inhibited with IMB-10 at a 20 μM concentration, whereas 20 μM gelatinase-selective inhibitor (InhI) reduced the proteolysis of uPAR (Figure 5D). Thus, gelatinase-mediated proteolysis is insensitive to the IMB-10 treatment, and the observed inhibition of migration is not caused by defective proteolysis.

Suppression of Inflammation in Vivo. As leukocyte integrins are needed for proper inflammatory response, we tested the functionality of IMB-10 in thioglycolate-induced peritonitis in mice. In this model, the DDGW peptide potently inhibits the emigration of activated neutrophils into the peritoneal cavity (*14*). At a dose of 4 μg of intravenously injected IMB-10, the number of leukocytes in the peritoneum was reduced by 70% 3 h after induction of inflammation. IMB-8 did not inhibit the neutrophil accumulation (Figure 6A). After 24 h the number of leukocytes was reduced essentially to background levels by IMB-10 but not by IMB-8 (Figure 6A). Approximately 50−60% of the emigrated cells were neutrophils after 24 h, the rest of the cells consisting mainly of macrophages and T cells. These data indicate that the IMB-10 is sufficiently potent and stable to inhibit neutrophil emigration in vivo, although exact bioavailability of the compound remains to be analyzed.

DISCUSSION

We have developed a simple and sensitive high-throughput assay based on competition of peptide-displaying phage by small molecules. This allowed us to identify a novel class of compounds, which stabilize the active conformation of the integrin α_M I domain. The screening method described here allows a direct route for identification of small molecules to practically any target to which peptide ligands can be obtained.

The α_M integrin I domain-binding compounds identified are structurally and functionally distinct from the previously characterized α_M and α_L I domain ligands (*6*, *10*, *11*, *13*, *38*). IMB-10, the most potent of these compounds, caused a severalfold increase in the binding activity of the recombinant α_M I domain. Remarkably, IMB-10 made $\alpha_M\beta_2$-expressing cells highly resistant to detachment from the substratum by the cation chelator EDTA. We propose a model where IMB-10 shifts the equilibrium between the closed and open I domain conformations toward the open conformation. This leads to the observed increase in binding activity to physiological ligands such as fibrinogen and proMMP-9, which favor the open conformation. In contrast, some antibodies or peptides such as DDGW prefer the closed, inactive conformation, and thus their binding is inhibited. In this model, IMB-10 binds to the region analogous to that of lovastatin in the α_L I domain (*32*), with the exception that the binding site for IMB-10 in the α_M I domain is present only in the open conformation. The ligands we identified are elongated and hydrophobic molecules, and the best of these compounds, IMB-10, effectively provides a complementary surface to the cavity observed in the active integrin α_M I domain. This binding prevents the re-formation of the contacts between the C-terminal helix and this cavity, which is essential for the stabilization of the closed inactive conformation. The model further indicates that amino acid residues I^{236}, Y^{267}, I^{308}, and I^{312} form contacts with IMB-10, and their mutations change the shape of the IMB-10 binding pocket, consistent with the data that they all reduced the binding induced by IMB-10. However, we cannot formally exclude the possibility that the $I^{236}A$ and $Y^{267}A$ mutations, which had the most dramatic effect, could abolish the ability of the α_M I domain to adopt the open conformation. In addition, we confirmed that the K^{245} residue in the α_M I domain is critical for the high-affinity binding of MMP-9 to the α_M I domain. Interestingly, using intact integrins, the IMB-10 was found to be clearly superior to the other compounds, suggesting that the rest of integrin probably constrains the movement of the C-terminal helix and may make the binding of other identified chemicals less favorable.

Despite the inability to prevent ligand binding of the α_M I domain, IMB-10 was a highly potent inhibitor of leukemia cell migration in the transwell assay and leukocyte recruitment in the in vivo inflammation model. The IMB-10 compound selectively affected β_2 integrin-dependent migration, as there was no effect on the migration of HT1080 fibrosarcoma cells lacking these integrins. Furthermore, the ability of IMB-10 to inhibit leukemia cell migration on fibrinogen is independent of gelatinase activity as judged by the inability of the gelatinase-selective inhibitor (InhI) to block cell migration and that IMB-10 did not inhibit pericellular gelatinase-dependent proteolysis of uPAR. These data strongly suggest that the primary mechanism of IMB-10 on cell migration is due to stabilization of $\alpha_M\beta_2$ integrin-mediated adhesive contacts. However, it is still possible that IMB-10 could exert some of its effects by a yet unidentified mechanism, possibly caused by constitutive signaling mediated by the activated integrins. It has been observed that the lack of α_M does not prevent neutrophil migration in the peritonitis model (*39*), but ablation of α_L has a strong effect (*40*), and that neutrophil recruitment in wild-type mice can be only partially inhibited by monoclonal antibodies to α_M integrin. A combination of α_L and α_M antibodies is needed to completely abolish the migration (*41*). Hence, the effective inhibition of neutrophil emigration and the phage and antibody binding experiments with the α_L I domain indicate that IMB-10 may also be capable of modulating α_L functions.

The concept of increasing adhesion through stabilization of the active conformation of the integrins to prevent cell migration may offer several benefits compared to the use of integrin antagonists. Importantly, targeting of the activated integrins may confer selectivity toward those cells that have responded to the pathological stimulus. Furthermore, as the identified chemicals stabilize adhesion to the underlying matrix, the cells cannot compensate the resulting single integrin "deficiency" by utilizing other integrins for migration as can be observed with gene knockout models (*42*, *43*). In accordance with our findings, quantitative studies on cell migration have established that cell migration and its speed can be regulated by relatively small changes in integrin affinity to the ligand in a biphasic fashion; i.e., if the affinity of integrin to matrix is decreased or increased from the optimum, the speed of migration will drop (*44*). Similarly, overexpression of mutant integrins, which stabilize adhesion, results in migration defects (*45*). To detach under stabilized adhesion, the cells have to shift from integrin affinity modulation more to the membrane ripping mechanism, where integrins and membrane aggregates are left behind the migrating cell (*45*, *46*). As the rear release from the matrix is the rate-limiting factor for cell migration (*47*), more extensive utilization of membrane ripping would be a costly mechanism due to the necessity to replace the lost proteins and membrane lipids, resulting in a dramatic decrease of cell migration speed. The low cell migration rates seen in the presence of IMB-10 and high coating concentration of a matrix protein are thus consistent with such a model, although further work is needed for the complete validation of this model.

In conclusion, stabilization of the high-affinity conformation of the $\alpha_M\beta_2$ integrin by IMB-10 effectively prevents $\alpha_M\beta_2$-dependent cell migration in vitro and leukocyte recruitment in vivo. Although it has been recognized that integrin-activating antibodies and adhesion-stabilizing mutant integrins can cause defects in cell migration (*45*, *46*), there have been no small molecules that would work in a similar fashion. The compounds described here are the first representatives of this novel class of integrin blockers that may have a utility as antiinflammatory compounds.

ACKNOWLEDGMENT

We thank Carl G. Gahmberg for the β_2 integrin antibodies, Leena Kuoppasalmi for the purification of $\alpha_M\beta_2$ integrin, and Jaana Kekkonen for technical assistance.

SUPPORTING INFORMATION AVAILABLE

Three figures showing structures of the compounds inhibiting the DDGW-phage binding to the α_M I domain−GST fusion, a comparison of binding fitness of IMB-10 to the α_M and α_L I domains, and a structure−activity analysis of IMB-10. This material is available free of charge via the Internet at http://pubs.acs.org.

REFERENCES

1. Hynes, R. O. (2002) Integrins: bidirectional, allosteric signaling machines, *Cell 110*, 673−687.

2. Xiong, J. P., Stehle, T., Diefenbach, B., Zhang, R., Dunker, R., Scott, D. L., Joachimiak, A., Goodman, S. L., and Arnaout, M. A. (2001) Crystal structure of the extracellular segment of integrin alpha Vbeta3, *Science 294*, 339−345.
3. Xiong, J. P., Stehle, T., Zhang, R., Joachimiak, A., Frech, M., Goodman, S. L., and Arnaout, M. A. (2002) Crystal structure of the extracellular segment of integrin alpha Vbeta3 in complex with an Arg-Gly-Asp ligand, *Science 296*, 151−155.
4. Salas, A., Shimaoka, M., Kogan, A. N., Harwood, C., von Andrian, U. H., and Springer, T. A. (2004) Rolling adhesion through an extended conformation of integrin alphaLbeta2 and relation to alpha I and beta I-like domain interaction, *Immunity 20*, 393−406.
5. Ruoslahti, E. (1996) RGD and other recognition sequences for integrins, *Annu. Rev. Cell Dev. Biol. 12*, 697−715.
6. Shimaoka, M., Salas, A., Yang, W., Weitz-Schmidt, G., and Springer, T. A. (2003) Small molecule integrin antagonists that bind to the beta2 subunit I-like domain and activate signals in one direction and block them in the other, *Immunity 19*, 391−402.
7. Luo, B. H., Takagi, J., and Springer, T. A. (2004) Locking the beta3 integrin I-like domain into high and low affinity conformations with disulfides, *J. Biol. Chem. 279*, 10215−10221.
8. Beglova, N., Blacklow, S. C., Takagi, J., and Springer, T. A. (2002) Cysteine-rich module structure reveals a fulcrum for integrin rearrangement upon activation, *Nat. Struct. Biol. 9*, 282−287.
9. Last-Barney, K., Davidson, W., Cardozo, M., Frye, L. L., Grygon, C. A., Hopkins, J. L., Jeanfavre, D. D., Pav, S., Qian, C., Stevenson, J. M., Tong, L., Zindell, R., and Kelly, T. A. (2001) Binding site elucidation of hydantoin-based antagonists of LFA-1 using multidisciplinary technologies: evidence for the allosteric inhibition of a protein−protein interaction, *J. Am. Chem. Soc. 123*, 5643−5650.
10. Liu, G., Huth, J. R., Olejniczak, E. T., Mendoza, R., DeVries, P., Leitza, S., Reilly, E. B., Okasinski, G. F., Fesik, S. W., and von Geldern, T. W. (2001) Novel p-arylthio cinnamides as antagonists of leukocyte function-associated antigen-1/intracellular adhesion molecule-1 interaction. 2. Mechanism of inhibition and structure-based improvement of pharmaceutical properties, *J. Med. Chem. 44*, 1202−1210.
11. Weitz-Schmidt, G., Welzenbach, K., Brinkmann, V., Kamata, T., Kallen, J., Bruns, C., Cottens, S., Takada, Y., and Hommel, U. (2001) Statins selectively inhibit leukocyte function antigen-1 by binding to a novel regulatory integrin site, *Nat. Med. 7*, 687−692.
12. Goodman, S. L., Holzemann, G., Sulyok, G. A., and Kessler, H. (2002) Nanomolar small molecule inhibitors for alphav(beta)6, alphav(beta)5, and alphav(beta)3 integrins, *J. Med. Chem. 45*, 1045−1051.
13. Bansal, V. S., Vaidya, S., Somers, E. P., Kanuga, M., Shevell, D., Weikel, R., and Detmers, P. A. (2003) Small molecule antagonists of complement receptor type 3 block adhesion and adhesion-dependent oxidative burst in human polymorphonuclear leukocytes, *J. Pharmacol. Exp. Ther. 304*, 1016−1024.
14. Stefanidakis, M., Ruohtula, T., Borregaard, N., Gahmberg, C. G., and Koivunen, E. (2004) Intracellular and cell surface localization of a complex between alphaMbeta2 integrin and promatrix metalloproteinase-9 progelatinase in neutrophils, *J. Immunol. 172*, 7060−7068.
15. Stefanidakis, M., Bjorklund, M., Ihanus, E., Gahmberg, C. G., and Koivunen, E. (2003) Identification of a negatively charged peptide motif within the catalytic domain of progelatinases that mediates binding to leukocyte beta 2 integrins, *J. Biol. Chem. 278*, 34674−34684.
16. Björklund, M., and Koivunen, E. (2005) Gelatinase-mediated migration and invasion of cancer cells, *Biochim. Biophys. Acta 1755*, 37−69.
17. Koivunen, E., Arap, W., Valtanen, H., Rainisalo, A., Medina, O. P., Heikkila, P., Kantor, C., Gahmberg, C. G., Salo, T., Konttinen, Y. T., Sorsa, T., Ruoslahti, E., and Pasqualini, R. (1999) Tumor targeting with a selective gelatinase inhibitor, *Nat. Biotechnol. 17*, 768−774.
18. Koivunen, E., Ranta, T. M., Annila, A., Taube, S., Uppala, A., Jokinen, M., van Willigen, G., Ihanus, E., and Gahmberg, C. G. (2001) Inhibition of beta(2) integrin-mediated leukocyte cell adhesion by leucine-leucine-glycine motif-containing peptides, *J. Cell Biol. 153*, 905−916.
19. Pasqualini, R., Koivunen, E., Kain, R., Lahdenranta, J., Sakamoto, M., Stryhn, A., Ashmun, R. A., Shapiro, L. H., Arap, W., and Ruoslahti, E. (2000) Aminopeptidase N is a receptor for tumor-homing peptides and a target for inhibiting angiogenesis, *Cancer Res. 60*, 722−727.
20. Kay, B., Kurakin, A., and Hyde-DeRuyscher, R. (1998) From peptides to drugs via phage display, *Drug Discov. Today 3*, 370−378.
21. Hyde-DeRuyscher, R., Paige, L. A., Christensen, D. J., Hyde-DeRuyscher, N., Lim, A., Fredericks, Z. L., Kranz, J., Gallant, P., Zhang, J., Rocklage, S. M., Fowlkes, D. M., Wendler, P. A., and Hamilton, P. T. (2000) Detection of small-molecule enzyme inhibitors with peptides isolated from phage-displayed combinatorial peptide libraries, *Chem. Biol. 7*, 17−25.
22. Michishita, M., Videm, V., and Arnaout, M. A. (1993) A novel divalent cation-binding site in the A domain of the beta 2 integrin CR3 (CD11b/CD18) is essential for ligand binding, *Cell 72*, 857−867.
23. Bjorklund, M., Heikkila, P., and Koivunen, E. (2004) Peptide inhibition of catalytic and noncatalytic activities of matrix metalloproteinase-9 blocks tumor cell migration and invasion, *J. Biol. Chem. 279*, 29589−29597.
24. Rowsell, S., Hawtin, P., Minshull, C. A., Jepson, H., Brockbank, S. M., Barratt, D. G., Slater, A. M., McPheat, W. L., Waterson, D., Henney, A. M., and Pauptit, R. A. (2002) Crystal structure of human MMP9 in complex with a reverse hydroxamate inhibitor, *J. Mol. Biol. 319*, 173−181.
25. Li, R., Xie, J., Kantor, C., Koistinen, V., Altieri, D. C., Nortamo, P., and Gahmberg, C. G. (1995) A peptide derived from the intercellular adhesion molecule-2 regulates the avidity of the leukocyte integrins CD11b/CD18 and CD11c/CD18, *J. Cell Biol. 129*, 1143−1153.
26. Xiong, J. P., Li, R., Essafi, M., Stehle, T., and Arnaout, M. A. (2000) An isoleucine-based allosteric switch controls affinity and shape shifting in integrin CD11b A-domain, *J. Biol. Chem. 275*, 38762−38767.
27. Lee, J. O., Bankston, L. A., Arnaout, M. A., and Liddington, R. C. (1995) Two conformations of the integrin A-domain (I-domain): a pathway for activation?, *Structure 3*, 1333−1340.
28. Morris, G. M., Goodsell, D. S., Halliday, R. S., Huey, R., Hart, W. E., Belew, R. K., and Olson, A. J. (1998) Automated docking using a lamarckian genetic algorithm and an empirical binding free energy function, *J. Comput. Chem. 19*, 1639−1662.
29. Shimaoka, M., Xiao, T., Liu, J. H., Yang, Y., Dong, Y., Jun, C. D., McCormack, A., Zhang, R., Joachimiak, A., Takagi, J., Wang, J. H., and Springer, T. A. (2003) Structures of the alpha L I domain and its complex with ICAM-1 reveal a shape-shifting pathway for integrin regulation, *Cell 112*, 99−111.
30. McCleverty, C. J., and Liddington, R. C. (2003) Engineered allosteric mutants of the integrin alphaMbeta2 I domain: structural and functional studies, *Biochem. J. 372*, 121−127.
31. Huth, J. R., Olejniczak, E. T., Mendoza, R., Liang, H., Harris, E. A., Lupher, M. L., Jr., Wilson, A. E., Fesik, S. W., and Staunton, D. E. (2000) NMR and mutagenesis evidence for an I domain allosteric site that regulates lymphocyte function-associated antigen 1 ligand binding, *Proc. Natl. Acad. Sci. U.S.A. 97*, 5231−5236.
32. Kallen, J., Welzenbach, K., Ramage, P., Geyl, D., Kriwacki, R., Legge, G., Cottens, S., Weitz-Schmidt, G., and Hommel, U. (1999) Structural basis for LFA-1 inhibition upon lovastatin binding to the CD11a I-domain, *J. Mol. Biol. 292*, 1−9.
33. Zhang, L., and Plow, E. F. (1999) Amino acid sequences within the alpha subunit of integrin alpha M beta 2 (Mac-1) critical for specific recognition of C3bi, *Biochemistry 38*, 8064−8071.
34. Lee, J. O., Rieu, P., Arnaout, M. A., and Liddington, R. (1995) Crystal structure of the A domain from the alpha subunit of integrin CR3 (CD11b/CD18), *Cell 80*, 631−638.
35. Shimaoka, M., Shifman, J. M., Jing, H., Takagi, J., Mayo, S. L., and Springer, T. A. (2000) Computational design of an integrin I domain stabilized in the open high affinity conformation, *Nat. Struct. Biol. 7*, 674−678.
36. Yakubenko, V. P., Lishko, V. K., Lam, S. C., and Ugarova, T. P. (2002) A molecular basis for integrin alpha Mbeta 2 ligand binding promiscuity, *J. Biol. Chem. 107*, 1.
37. Simon, D. I., Wei, Y., Zhang, L., Rao, N. K., Xu, H., Chen, Z., Liu, Q., Rosenberg, S., and Chapman, H. A. (2000) Identification of a urokinase receptor-integrin interaction site. Promiscuous regulator of integrin function, *J. Biol. Chem. 275*, 10228−10234.
38. Kelly, T. A., Jeanfavre, D. D., McNeil, D. W., Woska, J. R., Jr., Reilly, P. L., Mainolfi, E. A., Kishimoto, K. M., Nabozny, G. H.,

Zinter, R., Bormann, B. J., and Rothlein, R. (1999) Cutting edge: a small molecule antagonist of LFA-1-mediated cell adhesion, *J. Immunol. 163*, 5173−5177.

39. Lu, H., Smith, C. W., Perrard, J., Bullard, D., Tang, L., Shappell, S. B., Entman, M. L., Beaudet, A. L., and Ballantyne, C. M. (1997) LFA-1 is sufficient in mediating neutrophil emigration in Mac-1-deficient mice, *J. Clin. Invest. 99*, 1340−1350.
40. Ding, Z. M., Babensee, J. E., Simon, S. I., Lu, H., Perrard, J. L., Bullard, D. C., Dai, X. Y., Bromley, S. K., Dustin, M. L., Entman, M. L., Smith, C. W., and Ballantyne, C. M. (1999) Relative contribution of LFA-1 and Mac-1 to neutrophil adhesion and migration, *J. Immunol. 163*, 5029−5038.
41. Henderson, R. B., Lim, L. H., Tessier, P. A., Gavins, F. N., Mathies, M., Perretti, M., and Hogg, N. (2001) The use of lymphocyte function-associated antigen (LFA)-1-deficient mice to determine the role of LFA-1, Mac-1, and alpha4 integrin in the inflammatory response of neutrophils, *J. Exp. Med. 194*, 219−226.
42. Berlin-Rufenach, C., Otto, F., Mathies, M., Westermann, J., Owen, M. J., Hamann, A., and Hogg, N. (1999) Lymphocyte migration in lymphocyte function-associated antigen (LFA)-1-deficient mice, *J. Exp. Med. 189*, 1467−1478.
43. Yang, J. T., and Hynes, R. O. (1996) Fibronectin receptor functions in embryonic cells deficient in alpha 5 beta 1 integrin can be replaced by alpha V integrins, *Mol. Biol. Cell 7*, 1737−1748.
44. Palecek, S. P., Loftus, J. C., Ginsberg, M. H., Lauffenburger, D. A., and Horwitz, A. F. (1997) Integrin-ligand binding properties govern cell migration speed through cell-substratum adhesiveness, *Nature 385*, 537−540.
45. Geuijen, C. A., and Sonnenberg, A. (2002) Dynamics of the alpha6beta4 integrin in keratinocytes, *Mol. Biol. Cell 13*, 3845−3858.
46. Regen, C. M., and Horwitz, A. F. (1992) Dynamics of beta 1 integrin-mediated adhesive contacts in motile fibroblasts, *J. Cell Biol. 119*, 1347−1359.
47. Palecek, S. P., Huttenlocher, A., Horwitz, A. F., and Lauffenburger, D. A. (1998) Physical and biochemical regulation of integrin release during rear detachment of migrating cells, *J. Cell Sci. 111*, 929−940.

BI052238B